

Evaluation of thermal performance of window materials for satellite payloads in low earth orbit (LEO)

Andrew Baloyi^{1*}, Realeboga Dikole¹, Shrikant Naidoo¹, and Rofhiwa Seletani¹

¹Council for Scientific and Industrial Research (CSIR), Optronics Sensor Systems (OSS), PO Box 395, 0001, South Africa

Abstract. Selecting the appropriate window materials for use in space products such as Low Earth Orbit (LEO) satellite optical payloads is of critical importance. Windows on satellite optical payloads are essential for mission success and functionality. They serve a dual purpose: shielding the optical instrument's interior from environmental hazards and physical damage, while allowing beneficial radiation to pass through, ensuring optimal performance. However, temperature gradients can deform an inherently plane-parallel window and turn it into a weak meniscus, introducing Optical Path Difference (OPD) into the wavefront. This may lead to defocusing, thereby reducing the payload's performance. Design considerations to account for thermal stresses to prevent window damages such as "cracking", "crazing" and "delamination" due to "thermal cycling" are vital. This paper analyses the thermal performance of ULE Corning 7972 and Fused Silica window materials for LEO satellite optical payloads, considering solar radiation, Earth's Albedo (solar reflection), and Earth infrared radiation. ULE Corning 7972 outperformed Fused Silica due to its near-zero CTE, exhibiting less deformation and lower thermal stress. This analysis offers valuable insights into window material selection for enhanced reliability, durability, and functionality for LEO satellite optical payloads.

1 Introduction

Selecting appropriate materials for space product design is a vital step in the development process, ensuring optimal performance, durability, resilience, and mission success in the extremes of the space environment. Materials used in the construction of space products, including satellite optical payloads designed for LEO operations, must withstand the extreme conditions of space to ensure mission success. This is because the space environment is significantly harsher compared to Earth, owing to the lack of atmospheric protection from ultraviolet (UV) radiation, "atomic oxygen," "protons," and "electrons [3]. Consequently,

* Corresponding author: abaloyi3@csir.co.za

these materials must be carefully selected, considering their engineering properties and the specific requirements of the satellite's mission to ensure optimal performance and durability [2].

Windows on optical payloads, designed to transmit valuable electromagnetic radiation, must also meet stringent requirements to maintain their optical integrity and performance in demanding space environments. Among these requirements are high mechanical strength, robustness, resilience to endure impact damages, resistance to thermal shocks, durability in harsh environmental conditions, and light weight [1]. This research offers an in-depth thermal evaluation aimed at assessing the thermal characteristics of two window materials intended for utilisation in optical payloads on LEO satellites. The materials under consideration are ULE Corning 7972 and Fused Silica (FS). This analysis incorporates the following load combinations; the Sun's solar radiation, the Earth's reflected energy (Albedo), and infrared radiation (IR) from the Earth [2]. This thermal analysis offers essential insights into the design and selection of window materials for LEO satellite optical payloads to guarantee reliability, durability, and performance.

The study will use the typical expected operating conditions of the Potassium (K)-line satellite CubeSAT, ZACUBE3, currently under development by the Council for Scientific and Industrial Research (CSIR). The ZACUBE3 satellite is a fire detection satellite designed to operate at low Earth orbit at an altitude of 500 km and an inclination of 97.4° [17]. The orbital period of the satellite is 94 minutes, with a sun synchronous orbit. ULE Corning 7972 Ultra Low Expansion glass is a titania silicate glass possessing distinctive features that have established it as a preferred material for uses in "large astronomical telescope mirror blanks" and space satellite applications [5]. Its "near zero" coefficient of thermal expansion ($0.3 \times 10^{-7}/^{\circ}\text{C}$) (CTE) means that the material will exhibit low thermal deformations and stresses, attributes that are key for optimal performance of optical systems [5]. The glass material (ULE Corning 7972) also possesses good optical properties, with a refractive index of 1.4801 in the visible spectrum [4].

For a considerable time, Fused Silica (FS) has been the material of choice for building windows used in space applications [2]. The glass also has a moderate refractive index of 1.456 in the visible spectrum as shown in Table 1. It also possesses a significantly low coefficient of thermal expansion ($0.55 \times 10^{-6}/^{\circ}\text{C}$), which consequently results in minimal thermal stresses [2]. The glass also possesses excellent transmittance of ultraviolet radiation [2]. As per [2], this glass allows nearly all solar and Earth's reflective energy (Albedo) to pass through with minimal absorption, while it absorbs "Earth's infrared radiation" (IR). When choosing window materials for optical payloads, it's important to consider that windows, as optical components, are not shielded from space environmental conditions since they need to transmit critical radiation to the payload's sensors to fulfil their missions [2]. As such, selected window materials need to offer an excellent balance between performance and resistance to various space environmental conditions and loads such as thermal cycling.

The ZACUBE3 satellite is set to operate in a sun-synchronous orbit, which means it will constantly face the Sun, ensuring that the solar radiation it receives remains constant. Also, since the ZACUBE3 satellite operates in LEO, it will be exposed to direct radiation from the Sun, the reflection from Earth's surface (Albedo), and the infrared radiation (IR) emitted by Earth [2]. These radiations will have a significant impact on the satellite's structural materials, especially windows, as they cannot be shielded from radiation sources. It is therefore the objective of this study to evaluate the thermal performance of the two window materials (ULE Corning 7972 and Fused Silica), which both possess excellent engineering properties for use in the space environment.

The remainder of the paper is organised as follows: Section 2 addresses the related work conducted on similar topics and outlines the contribution of this work to the current body of knowledge, Section 3 provides an overview of the conventional celestial reference frame of

an orbiting body, Section 4 addresses the variability of the radiation sources experienced by the satellite, Section 5 outlines the methodology adopted, Section 6 discusses results and findings of the study and lastly Section 7 outlines conclusions and recommendations for future research.

2 Related work

From the reviewed literature, research has specifically concentrated on determining and calculating the “operating temperatures” of “transparent window materials” in the space environment, such as [2]. These operating temperatures are a function of transmittance, absorptivity and reflectivity of window materials to various radiations in space. A comparative study conducted by [2] between Fused Silica and Acrylic glass, found that acrylic glass resulted in higher operating temperatures due to its higher absorptivity.

Other studies, such as [7-10], have examined the operating temperatures of satellites in space, treating them as independent units to assess their thermal performance and behaviour in extreme environments. This study will focus on understanding the impact these temperatures have on the physical dimensions and form of the window materials when exposed to the combination of direct solar heat flux, Earth’s albedo and Earth’s infrared radiation (IR). This is crucial because any deviation in an optical element’s original physical dimensions could lead to an optical system partially or completely failing to accomplish its mission. As far as we are aware, this analysis offers a unique addition to the existing body of knowledge relating to the analysis of windows used in space environments.

3 Celestial reference frame of a body in orbit

Figure 1 illustrates a typical Celestial Reference Frame, also known as the Earth-Centred Inertial, which is centred at the “geocentre” [2]. The ecliptic plane is inclined at an angle, $\psi = 23.45^\circ$, relative to the Earth’s equatorial plane, and it is the plane where the sun vector \mathbf{o} lies, as illustrated in Figure 1(a). Figure 1(b) shows the orbital plane of the ZACUBE3 satellite at an inclination angle of $\phi = 97,3^\circ$ to the equatorial plane. The “beta angle,” denoted by β , is the angle formed between the satellite’s orbital plane and the ecliptic plane, determining the extent of “shadowing” experienced by the orbiting object in space [2]. The beta angle plays a significant role in the heat transfer rates experienced by the orbiting object in space, and it varies between $\pm 75^\circ$ yearly [7].

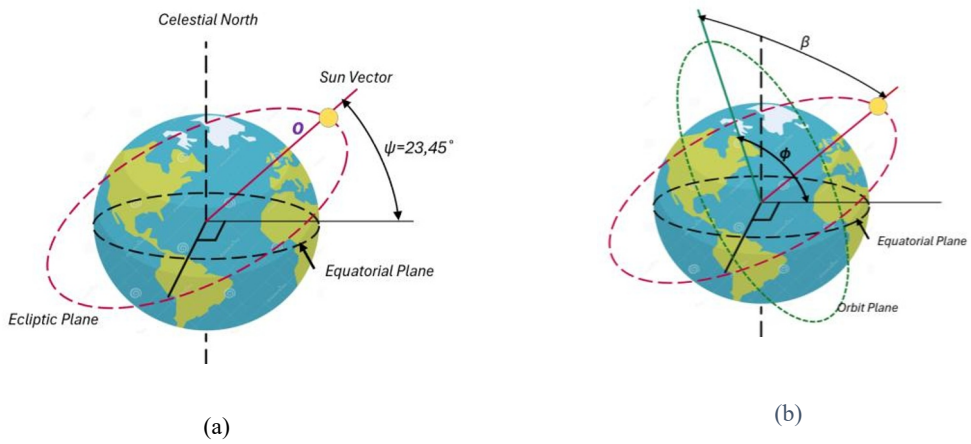


Fig. 1. (a) Celestial Reference Frame of an orbiting body, and (b) satellite's orbiting plane and the "beta angle", β [2].

4 ZACUBE3 satellite radiation sources variability

The amount of radiation anticipated on the ZACUBE3 satellite's optical window will be proportional to the satellite's position and orientation in space. The three sources of radiation, namely solar radiation, Earth's albedo radiation, and Earth's infrared radiation, will also change over time due to the satellite's orbiting motion [2]. ZACUBE3 satellite's orbital period T was calculated to be 94 minutes as shown by Equation 1.

$$T = 2 \times \sqrt{\frac{(R + H)^3}{GM}} \quad (1)$$

Where R = radius of the earth, H = satellite's altitude, M = mass of the earth and G = universal gravitational constant. The values for R , H , M and G are 6873km, 500km, $5.95 \cdot 10^{24}$ kg and $6.67 \cdot 10^{-11}$ m³/kg · s², respectively. Figure 2 shows the "umbral or eclipse region", where the sun does not reach, and the "penumbral region" which is the area that some of the sun's rays partially reach [2]. As the LEO satellite orbits the earth, it will eventually find itself spending some time in these two regions during its orbit. The amount of time spent in each region is dependent on the beta angle, β . As stated in [7], beta angles less than 90° correspond to a higher eclipse fraction, and the satellite will spend most of its time in the eclipse or umbral region, see Figure 2. The eclipse fraction determines the duration for which the satellite is subjected to any of the three heat flux sources [7]. This means that the only heat flux experienced by the satellite when in the eclipse region is the infrared radiation from the earth, both solar and albedo will be zero [2].

For beta angles greater than 90°, the eclipse fraction converges to zero, and the satellite will spend most of its time in the penumbral region, see Figure 2. This means that it will experience heat flux from all the three sources (solar radiation, albedo and infrared radiation) when in this region. The beta angle that defines the transition of the satellite from umbral to penumbral regions or vice-versa is called critical beta angle, β^* [2]. This angle is calculated using Equation 2. For ZACUBE3 satellite, the critical beta angle was found to be 68.77°. This angle results in a piece-wise function, presented in Equation 3, that characterizes the

proportion of time the satellite spends within the umbral region [7]. The plot of the piecewise function is illustrated by Figure 3.

$$\beta^* = \arcsin\left(\frac{R}{R+H}\right) \quad (2) [7]$$

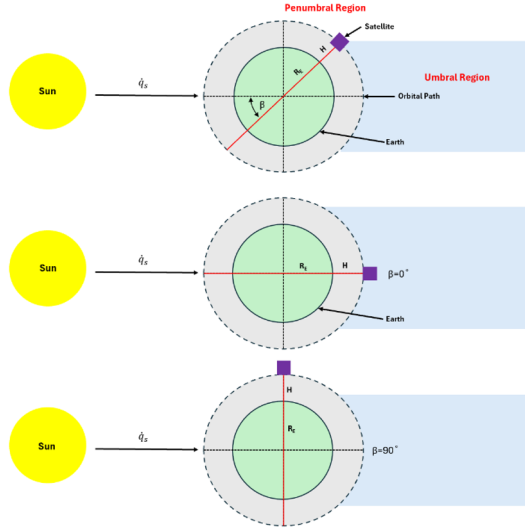


Fig. 2. Beta angle (β) variation, Umbral and Penumbral regions.

$$Ef = \begin{cases} \frac{1}{180^\circ} \cos^{-1}\left(\frac{\sqrt{H^2 + 2RH}}{(R+H)\cos(\beta)}\right), & |\beta| < \beta^* \\ 0, & |\beta| \geq \beta^* \end{cases} \quad (3)$$

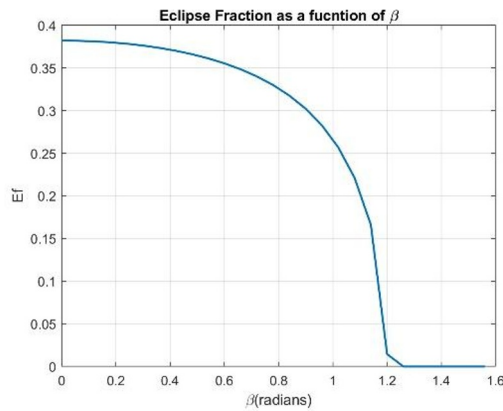


Fig. 3. Eclipse Fraction as a function of beta angle, β .

5 Methodology

5.1 Window materials thermal properties

As discussed in section 1, the two windows were constructed from ULE Corning 7972 and Fused Silica glass materials. The window geometry dimensions are diameter, $d=180\text{mm}$ and thickness, $x=13\text{mm}$. Figure 4 is an illustration of the window geometry used for conducting the thermal analysis. Both these materials possess excellent thermal and optical properties as outlined in Table 1. The window geometry was given the material properties of both ULE Corning 7972 and Fused Silica during the analysis. The properties of the two window materials are summarised in Table 1 for reference.

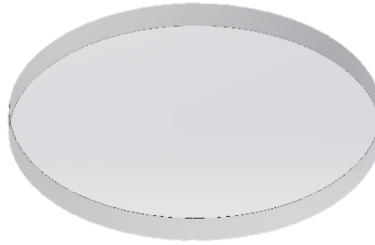


Fig. 4. Window geometry used for FEA.

Table 1. Thermal, mechanical and optical properties of ULE Corning 7972 and fused silica [4, 6].

Thermal Property	ULE Corning 7972	Fused Silica
Coefficient of Thermal Expansion (α)	$0.3 \times 10^{-7}/^{\circ}\text{C}$	$0.55 \times 10^{-6}/^{\circ}\text{C}$
Thermal Conductivity (K)	$1.31 \text{ W/m}^{\circ}\text{C}$	$1.38 \text{ W/m}^{\circ}\text{C}$
Specific Heat Capacity (C_p)	$767 \text{ J/kg}^{\circ}\text{C}$	$740 \text{ J/kg}^{\circ}\text{C}$
Mechanical Property		
Poisson's ratio	0.17	0.17
Ultimate Tensile Strength	49.8 MPa	48 MPa
Density	2.21 g/cm^3	2.2 g/cm^3
Elastic Modulus	67.6 GPa	73 GPa
Bulk Modulus	41 GPa	34.1 GPa
Optical Property		
Refractive index	1.4801 (656nm)	1.456 (650nm)

5.2 Heat flux model

The heat flux model incorporated the solar heat flux, Earth’s albedo and the infrared radiation (IR) emitted by the Earth. Another critical function governing the heat flux experienced by the satellite in orbit is the solar heat flux multiplier function, i.e. \hat{s} . The solar heat flux multiplier function will ensure that the heat flux model removes the solar and albedo heat fluxes during the times when the satellite enters the eclipse region and brings them back when the satellite enters the penumbral region [7]. Equation 4 is an illustration of the “solar heat flux multiplier”, which is a function of the orbital period T , and the eclipse fraction Ef [7].

$$\hat{s} = \begin{cases} 1 & \frac{T}{2}(1 - Ef) > t > \frac{T}{2}(1 + Ef) \\ 0 & \text{else} \end{cases} \quad (4)$$

Equation 5 illustrates the modified heat flux model from [7], where \dot{q}_{tot} is the total heat flux, \dot{q}_{IR} is the earth’s infrared radiation (IR), \dot{q}_{gen} is the heat generated inside the satellite, a is the albedo parameter, \dot{q}_s is the solar heat flux from the sun/ solar irradiance/ solar constant, and \hat{s} is the solar heat flux multiplier. The value for a can be taken to be 0.3 for computational purposes as stated in [2].

For \dot{q}_{IR} , a value of 218W/m^2 can be used for $\beta \geq 30^\circ$ [7]. The value of \dot{q}_s can be taken as 1367W/m^2 [7]. The heat generated was taken as 15W , corresponding to ZACUBE3’s anticipated nominal power budget. The component for radiation emitted by the window was omitted in the heat flux model. This is because given that $\tau(\lambda, T) + \rho(\lambda, T) + \alpha(\lambda, T) = 1$, and $\varepsilon(\lambda, T) = \alpha(\lambda, T)$ from conservation of energy and Kirchhoff’s law, it suffices to consider emissivity $\varepsilon(\lambda, T)$ to be negligible [9]. This can be seen from the fact that for non-opaque materials, $\rho(\lambda, T) \sim 0$, and $\tau(\lambda, T)$ is close enough to unity, thus the quantity $\varepsilon(\lambda, T) = 1 - \tau(\lambda, T)$ is close enough to zero [9]. The model was run in MATLAB, and the plot of the total heat flux as a function of time is shown Figure 5 below. The maximum heat flux experienced by the satellite was found to be 2010W/m^2 for the 94 minutes period.

$$\dot{q}_{tot} = \dot{q}_{IR} + \dot{q}_{gen} + (1 + a)\dot{q}_s\hat{s} \quad (5)$$

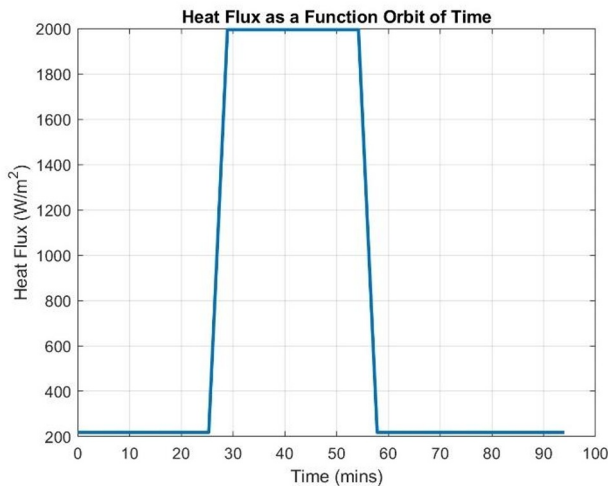


Fig. 5. Heat flux as a function of time.

5.3 Finite element analysis (FEA)

Finite Element Analysis (FEA) was adopted in conducting the thermal simulation on the windows. ANSYS Mechanical was used to conduct the simulation. Both transient and steady state simulations were conducted. Firstly, a transient analysis was performed to determine whether the window achieves a steady-state temperature within the satellite's 94-minute period. Secondly, steady state analysis was conducted, and the temperature results were compared to that of transient analysis. The analysis was conducted using three dimensional four – node tetrahedral elements. The materials were considered isotropic to ensure uniform heat transfer in every direction.

5.3.1 Mesh

The mesh consisted of four – node tetrahedral elements as stated in section 5.3. The number of nodes and elements were 32724 and 6684 respectively. Figure 6 illustrates the FEA mesh model.

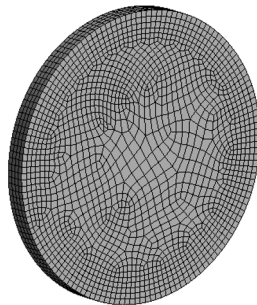


Fig. 6. FEA mesh model.

5.3.2 Boundary conditions

The window consisted of three constraints, i.e., two thermal (temperatures) and one structural (fixed). A fixed constraint on the window edge was selected because fastening or clamping the window edge to the satellite's structure minimizes deflections and stresses [1]. This differs from scenarios involving a simply supported window. For the temperature constraint on the window edge, a room temperature of 22°C was applied. It was also assumed that the ZACUBE3 thermal management system can maintain an internal temperature of 22°C, and therefore a thermal constraint of 22°C was applied to the internal face of the window, see Figure 7 (a). A fixed constraint was applied to the outer edge of the window, see Figure 7 (b). A heat flux load, $\dot{q}_{tot} = 2010\text{W/m}^2$ obtained from the heat flux model derived in Section 5.2 was applied on the opposite face (external) of the window. Figure 8 is an illustration of the heat flux load application on the external window face.

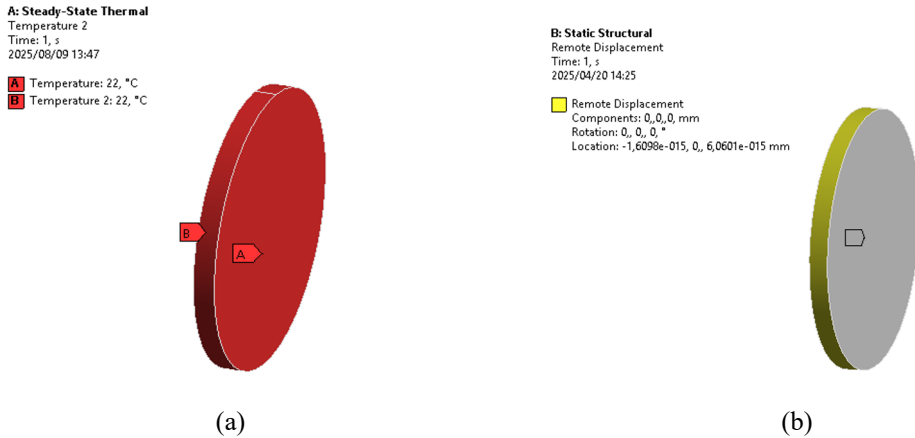


Fig. 7. (a) Temperature constraints on the internal face and on the edge of the window. (b) Fixed constraint on the window edge.

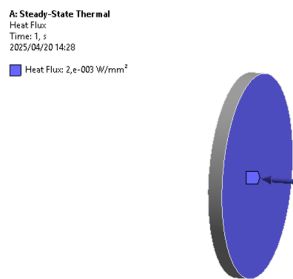


Fig. 8. Heat flux loading on the external face of the window.

6 Results

The results of the thermal simulation are summarised in Table 2 below. Both transient and steady state thermal analysis converged to the same steady temperature as shown in Figure 9 and Figure 11. This suggests that the 94-minute satellite period was sufficient for the window to achieve a steady-state temperature during the transient thermal analysis, and therefore our steady state thermal analysis temperatures are accurate. While ULE Corning 7972 material exhibited a somewhat elevated temperature relative to Fused Silica, it demonstrated significantly low total deformation and equivalent stress. ULE Corning 7972's deformation is seventeen (17) times lower than that of FS, which is a significant difference.

The equivalent stress is also significantly lower, and it is eighteen (18) times lower than that of FS. The findings indicate that ULE Corning 7972 exhibits superior thermal performance in comparison to FS. However, as illustrated in Table 2, the stresses on both window materials are considerably lower than their respective tensile strengths. Figures 9 – 12 illustrate the temperature, total deformation and equivalent stress contours of the two glass materials. The contours are in a slightly exaggerated format to illustrate how they deformed when exposed to the heat flux. These deformations are significantly small for a human eye to comprehend as seen in Table 2 below.

Table 2. Thermal simulation results.

Parameter	ULE Corning 7972	Fused Silica
Temperature	41,8°C	40,8°C
Total Deformation	0,000172mm	0,0030mm
Equivalent Stress (Von Mises)	0,0332MPa	0,624MPa

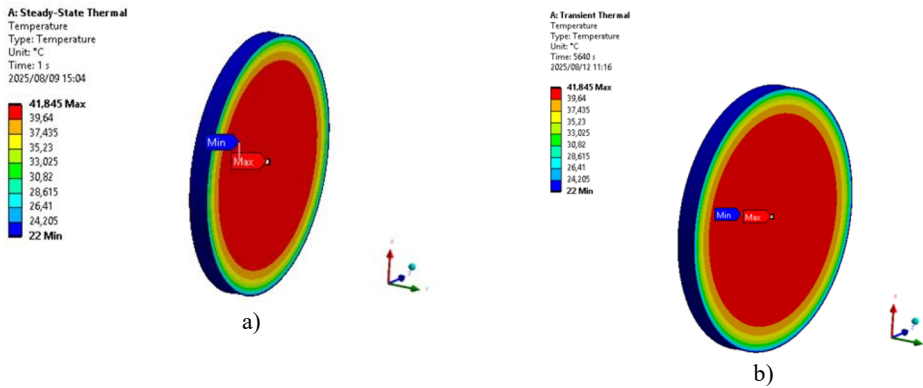


Fig. 9. (a) ULE Corning 7972 steady state temperature contour (steady state thermal analysis). (b) ULE Corning 7972 steady state temperature contour (transient thermal analysis).

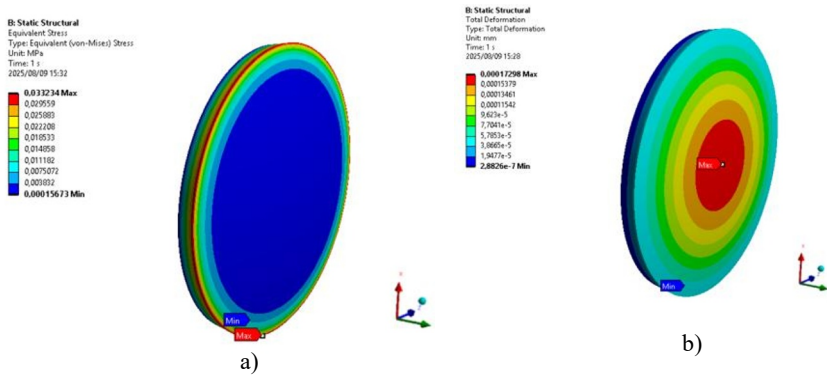


Fig. 10. (a) ULE Corning 7972 equivalent stress contour. (b) ULE Corning 7972 total deformation contour.

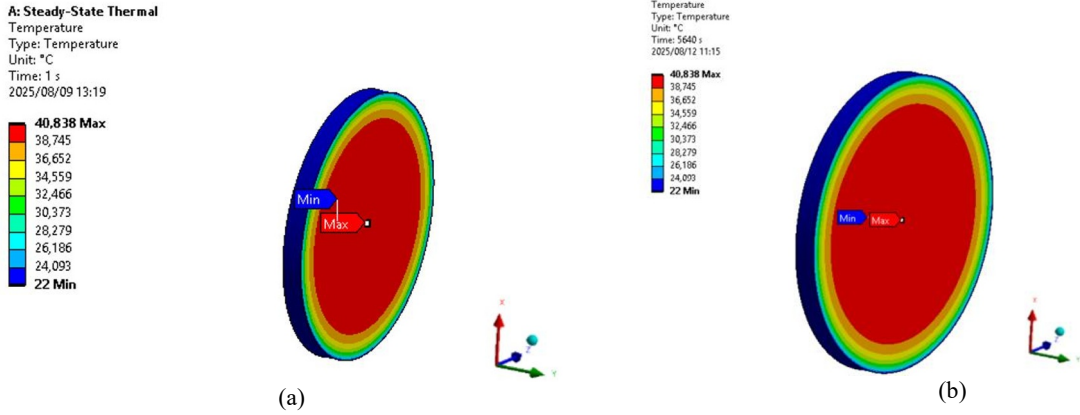


Fig. 11. (a) FS steady state temperature contour (steady state thermal analysis). (b) FS steady state temperature contour (transient thermal analysis).

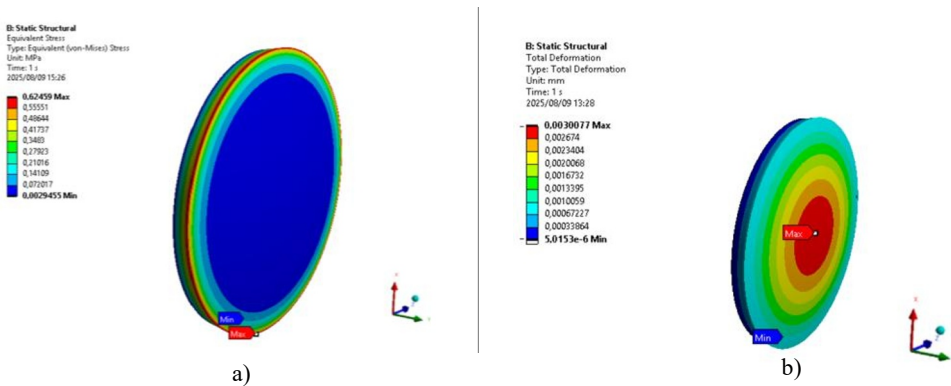


Fig. 12. (a) Fused Silica equivalent stress contour. (b) Fused Silica total deformation contour.

As stated in [1], when an “initially plane parallel” window deforms due to temperature gradients, OPD is introduced into the wavefront. Table 3 illustrates the OPD calculated results for both window materials using Equation 5 [1]. Using the maximum in-plane temperature gradient results obtained from the simulation, the results indicated that both window materials exhibited OPD values that are significantly lower than the limit of $\lambda/8$ [1], with ULE Corning 7972 exhibiting an even lower OPD value compared to FS.

$$OPD = nh\Delta T_{max} = \left(\alpha + \frac{1}{n} \frac{dn}{dT} \right) \quad (5)$$

Table 3. Optical path difference (OPD) results.

Parameter	Formula	ULE Corning 7972	Fused Silica
Refractive index	n	1.4801 (0.656μm)	1.456 (0.650μm)
Wavelength	λ	0.656μm	0,650μm
Coefficient of thermal expansion	α	3.0e-8/C	5.5e-7/C
Change in refractive index with temperature	dn/dT	1.124e-5/C	1.29e-5/C
Maximum in plane temperature gradient	ΔT _{max} = T _{max} - T _{min}	19.847°C	18.841°C
Window thickness	h	13mm	13mm
Optical Path Difference (OPD)	OPD =nhΔT _{max} =(α+ 1/n dn/dT)	2.9e-3μm	3.4e-3μm

7 Conclusion and recommendations

In this paper, we compared the thermal performances of two window materials for use on satellite optical payloads in LEO. The window materials are ULE Corning 7972 and Fused Silica. The comparison was focused on establishing the thermal performance of these materials, specifically deformation and thermal stresses when exposed to the space environment thermal loads. Windows are typically regarded as optical components with no power. However, if they experience significant deformation, they can act as weak meniscus lenses and cause an optical path difference (OPD) in the wavefront [1].

This phenomenon can degrade the performance of an optical system significantly. Excessive deformation due to temperature gradients does not only induce OPD into the wave front but could also induce thermal stresses that could crack the window depending on the severity of the stresses. The thermal results indicated that the two window materials exhibited very low deformations and thermal stresses, with ULE Corning 7972 outperforming FS. The lower deformations were due to the material’s low coefficients of thermal expansions, which then resulted in OPD’s that were much lower than the acceptable limit as outlined in Table 3, and therefore could be ignored. The two window materials are therefore suitable for use in satellite optical payloads: with ULE Corning 7972 being the most suitable given its much lower OPD compared to FS.

Due the unavailability of absorptivity, transmittivity and reflectivity data on ULE Corning 7972 in the literature and OEM’s data, these properties were not incorporated in the thermal simulation of the two materials. For FS, these properties were obtained using Maxwell’s equations of electromagnetism with respect to the solar and albedo radiation [11]. The same approach could be adopted to obtain the same properties for ULE Corning 7972 to be incorporated in the thermal analysis. However, for this research work, their incorporation in the thermal analysis would not have influenced the results given that the thermal equation is independent of these parameters as per Equation 6. Transient effects on the window as the satellite transition from umbral to penumbral regions and back were also not incorporated for this research work due to the software capability limitations. This analysis is thus recommended for future research.

$$\frac{\partial}{\partial x} \left(k \frac{\partial T}{\partial x} \right) + \left(k \frac{\partial T}{\partial y} \right) + \left(k \frac{\partial T}{\partial z} \right) + \dot{e}_{gen} = \rho c_p \frac{\partial T}{\partial t} \quad (6) [13]$$

Where:

- k is the thermal conductivity of the material (W/m.K)
- e is the heat generation rate per unit volume of the material (W/m³)
- ρ is the material's density (kg/m³)
- c_p is the specific heat capacity of the material (J.kg/K)

References

1. D. Vukobratovich and P. Yoder, *Fundamentals of Optomechanics* (CRC Press, 2018)
2. L. Galuppi, G. Royer-Carfagni, *Thermal Analysis of Space Station Windows in Low Earth Orbit: Intermaterial Comparison of Fused Silica and Acrylic Glass*, *Aero. Mis. & Spaz.* **26**, 1-20 (2025).
<https://doi.org/10.1007/s42496-025-00250-y>
3. L. Galuppi, G. Royer-Carfagni, *Thermo-optical modelling of transparent multilayer panels for Space Applications in Low Earth Orbit*, (2025)
4. Corning, 7972 ULE Product Information Jan 2016, January 2016. [Online]. Available: <https://www.corning.com/media/worldwide/csm/documents/7972%20ULE%20Product%20Information%20Jan%202016.pdf>. [Accessed 23 March 2025].
5. R. Sabia, M. J. Edwards, R. VanBrocklin, B. Wells, *Corning 7972 ULE material for segmented and large monolithic mirror blanks*, *Optomech. Tech. for Astron.* **6273**, 12-19 (2006)
doi: 10.1117/12.672059
6. R. Brucker, *Properties and Structure of vitreous silica. I*, *Journal of Non-Crystalline Solids*, 123-175 (1970)
7. C. Versteeg, D. Cotten, *Preliminary thermal analysis of small satellites*, The University of Georgia, Athens (2018)
8. V. Alcayed, A. Vercher-Martinez, F. J. Fuenmayor, *Thermal control of a spacecraft: Backward-implicit scheme programming and coating materials analysis*, *Adv. Space. Res.* **68**, 1975-1988 (2021)
<https://doi.org/10.1016/j.asr.2021.03.041>
9. M. Bonnici, M. Pierluigi, F. Maurizio, A. A. March, *Analytical and numerical models for thermal related design of a new pico-satellite*, *Appl. Therm. Eng.* **59**, 113908 (2019).
<https://doi.org/10.1016/j.applthermaleng.2019.113908>
10. S. Corpio, M. Caldera, F. Nichele, M. Masoero, N. Viola, *Thermal design and analysis of a nanosatellite in low earth orbit*, *Acta. Astron.* **115**, 247-261 (2015).
<http://dx.doi.org/10.1016/j.actaastro.2015.05.012>
11. L. Galuppi, G. Royer-Carfagni, *Energy Absorption Through Radiation in Multilayer Windows for Spacecrafts*, *Aero. Mis. & Spaz.* 1-8, (2024).
<https://doi.org/10.1007/s42496-024-00233-5>
12. N. Azzali, M. Meucci, D. Rosa, L. S. L. Mercatelli, D. Sciti, E. Sani, *Spectral emittance of ceramics for high temperature solar receivers*, *Sol. Ene.* **222**, 74-83 (2021).

- <https://doi.org/10.1016/j.solener.2021.05.019>
13. Y. A. Cengel and A. J. Ghajar, Heat and Mass Transfer, Fundamentals and Applications (McGraw-Hall Education, New York, 2011)
 14. A. Elshaer, A. Soliman, M. Kassab, S. Mori, A.A. Hawwash, Thermal control of a small satellite in low earth orbit using phase change materials-based thermal energy storage panel, *Egypt. J. Rem. Sens. and Space. Sci.* **26**, 954-965 (2023).
<https://doi.org/10.1016/j.ejrs.2023.11.007>
 15. R. Vicente, G. Nogues, J. Niot, T. Wiertz, P. Contini, Impacts of laser cooling for low earth orbit observation satellites: An analysis in terms of size, weight and power, *Cryo.* **105**, 103000 (2020).
<https://doi.org/10.1016/j.cryogenics.2019.103000>
 16. ACCURATUS, "Fused Silica, SiO₂ Glass Properties," [Online]. Available: <https://accuratus.com/fused.html>. [Accessed 20 April 2025].
 17. ZACUBE-2 (South African CubeSat-2), July 2016. [Online]. Available: <https://www.eoportal.org/satellite-missions/zacube-2#zacube-2-south-african-cubesat-2>. [Accessed 18 September 2025].